Uplink Cluster-Based Radio Resource Scheduling for HetNet mMTC Scenarios

Abdelrahman Ramadan*, Nizar Zorba‖, and Hossam S. Hassanein‡
*ECE Department, Queen's University, Kingston, ON, Canada 20amr3@queensu.ca
‖EE Department Qatar University, Doha, Qatar. nizarz@qu.edu.qa
‡School of Computing, Queen's University, Kingston, ON, Canada hossam@cs.queensu.ca

GLOBECOM 2022 - 2022 IEEE Global Communications Conference | 978-1-6654-3540-6/22/$31.00 ©2022 IEEE | DOI: 10.1109/GLOBECOM48099.2022.10000921

***Abstract*— Current telecommunication networks face a surge in the number of connected Machine-type Communication (MTC) devices, creating an unprecedented disproportionate demand for existing resources, especially when working with a Heterogeneous Networks (HetNets). This demand cannot be addressed adequately as the infrastructure's transition process between different generations is slow. Fourth Generation (4G) relies on Orthogonal Multiple Access (OMA), where a single user can occupy the same sub-channel, Orthogonality offers interference-free communication but for normal loaded scenarios, but under performs in overloaded scenarios. Whereas Fifth Generation (5G) is targeting more spectral efficiency by using the Non-orthogonal Multiple Access (NOMA), allowing MTC devices to share the same resources in frequency and time. However, NOMA medium access techniques in general have a complex scheduler design as group users/devices with aligned correlations. In this study, we formulate and simulate a 4G/5G Uplink scheduler that is based on dual NOMA-OMA. The objective is to achieve a tangible improvement in the spectral and scheduling efficiency of the network. We are able to optimize the system under HetNet objectives and clustering constraints in overloaded scenarios, to examine the limitations of both NOMA and OMA in overloaded scenarios.**

***Index Terms*—Scheduling, resource allocation, heterogeneous networks, NB-IoT, poisson cluster processes, 4G, 5G/NR, PD-NOMA, OFDMA.**

I. Introduction

The stochastic densification of the entire network on multiple levels is one of the major motivations for improving the Spectral Efficiency (SE) of next-generation networks, including but not limited to Fifth Generation (5G) and already established standards like 4G and their variants. That entails a dynamic change in the number of base stations and users and is not limited to only human users but also Machine-Type Devices (MTDs). Beyond 5G networks are expected to support hundreds of millions of connected MTD [1]. This surge, in turn, led to the emergence of paradigms that try to tackle problems congenital to densification in communication networks, whether it is in time or frequency domains.

Currently deployed systems lack flexibility and adaptability, and are in ever-consistent need of upgrades and fixes, leading to unmet demand for higher Quality of Service (QoS) and efficiency. That is where dynamic Radio Resource Scheduling (RRS) becomes essential [2], as we can assign spectral resources to MTDs while achieving the minimum QoS requirements, whether they are in fairness, delay, or throughput.

Supporting a larger density of connections (e.g., bursty traffic from proximity sensors [2], [3]) per cell also means putting a larger load on 4G/5G channels [4], [5]. Moreover, heterogeneity paradigms remain as a big challenge [6], [7], which hold a significant impact on how we conceptualize the state of future networks, such as the Internet of Everything (IoE) [8]. The paradigm of radio resource allocation/scheduling is generally a non-convex NP-hard problem [9] and therefore computationally complex, particularly as the density of the network increases. Researchers have developed a range of centralized and distributed radio resource allocation algorithms (User-Pairing as in [10], or Game-based algorithms [11], [12], using various techniques such as weighted minimum mean square optimization, information-theoretic [13], and fractional programming [14]. [15] formulated an optimization problem constrained by properties of cluster process, they focused on maximizing performance for mMTC, and URLLC devices, however, they considered a single cell scenario and relied upon PD-NOMA for transmission. Thus, clustering was useful as it can mitigate some challenges introduced by the full-collision property of NOMA. In [16] the authors were trying to bridge the gap between Poisson point processes and tier-based HetNets. They developed models for HetNets for different types of BS and UE configurations, which resulted in a unified model for simulating the non-uniformity of BSs and UEs locations throughout the HetNets. We define heterogeneity in a network where users access the medium using two different techniques: Power-Domain Non-Orthogonal Multiple Access (PD-NOMA) and Orthogonal Frequency-Division Multiple Access (OFDMA), and we try to optimize their resources to satisfy the QoS requirements for the MTDs.

The novelty of this work is that we explore the possibility of deploying a dynamic RRS algorithm as a solution to the relaxed optimization problem. We also give an insight into network trends under heterogeneity constraints in a Narrow-Band Internet of Things (NB-IoT) framework. The problem at hand incorporates orthogonal and non-orthogonal multiple access, which will provide a perspective on how integration is realized in future networks.

Henceforth, the main contributions of this paper are as follows:

1) We set up a scenario that couples orthogonal and non-orthogonal multiple access techniques, while considering QoS requirements for MTDs.
2) We formulate a constrained Optimization Problem (OP) to maximize the sumrate of OFDMA and PD-NOMA connected MTDs.
3) We provide a Pareto optimal solution to a relaxed OP through a heuristic algorithm, where the formulated non-relaxed OP is NP-hard.
4) We develop a simulator that considers many features of standardized systems; we then test the simulator's performance and limitations under various scenarios.

The rest of the paper is organized as follows, Section II will give a holistic view of the system model along with an introduction to the scenario we are evaluating. In Section III we formulate our Dynamic RRS problem and provide a heuristic solution. We showcase our simulation results and discussions in Section IV. Finally we conclude this work in Section V.

II. System Model

We investigate a multi-cell scenario with one Small Base Station (SBS) in each cell center that supports massive MTC (mMTC) and is following NB-IoT standard specifications. We assume MTDs are stationary or with very limited mobility. We Denote $\boldsymbol{\mathcal{M}} = \{1, ..., M\}$ as the set of MTD. For uplink data transfer in a single Transmission Time Interval (TTI), where active devices share a single Physical Resource Block (PRB) every TTI. Each PRB has a bandwidth that is partitioned into a series of sub-channels $\boldsymbol{\mathcal{S}} = \{1, ..., S\}$, where a bandwidth of W will be allocated to each sub-channel. This can be translated into 48 or 12 sub-channels in NB-IoT commercial systems.

We propose HetNet Poisson cluster process (PCP) scheme by clustering MTDs in an NB-IoT network, where clusters are generated in simulation environment according to Matérn cluster process [16], where the daughter points are distributed uniformly within a circle centered around a parent point as shown in Fig. 1. For simplicity, we shall denote the Matérn cluster process as PCP. The PCP process could be defined as

$$\rho_u = \bigcup_{\Theta \in \rho_{\mathrm{p}_u}} \Theta + O_u^{\Theta}, \tag{1}$$

where ρ_{p_u} denotes the parent PPP of density λ_{p_u} and O_u^{Θ} represents the daughter point process, where each point at $s \in O_u^{\Theta}$ is i.i.d. around the cluster center $\Theta \in \rho_{\mathrm{p}_u}$, where the density of daughter point process is $\mathcal{D}_u$.

The MTDs (according to the PCP scheme), share each sub-channel resources and transceive non-orthognally i.e., multiple MTDs can share the same sub-channel resources or in an orthogonal manner in case they are accessing the medium using OFDMA. As a result, the devices are dispersed into PCP groups, we denote as $\boldsymbol{\mathcal{C}} = \{1, ..., C\}$ cluster sets. $\gamma_{s,c,b}$ is a binary indicator where sub-channel $s \in \boldsymbol{\mathcal{S}}$ is dedicated to group $c \in \boldsymbol{\mathcal{C}}$, hence $\gamma_{s,c,b} = 1$ if sub-channel s is allotted and zero otherwise. The MTDs use the same sub-channel for transmission, with transmit powers of $p_{s,m}$, respectively. As a result, the SBS receives a combined message from MTDs with additive noise $\mathcal{N}_0$ and interference in case the MTD is using PD-NOMA. We denote the point process of the u^{th} SBS tier as ρ_u, where ρ_u is the PCP ($\forall u \in \mathcal{U}_1$), where $\mathcal{U}_1$ is the index set of the SBS tiers being modeled as PCP. Defining the set of ranks (levels) in each PCP group as $\mathcal{U} = \{1, ..., u_{max}\}$, where u_{max} defines the maximum number of MTD that can be in the same group and thereby utilize the allotted sub-channels We assume that $\boldsymbol{\mathcal{C}} \times u_{max}$ is greater than the population of MTD. It is worth noting that the MTD with the highest rank

TABLE I: List of Symbol Notations and Description

Symbol	Definition
$\boldsymbol{\mathcal{M}}$	The set of MTDs
$\boldsymbol{\mathcal{S}}$	The set of sub-channels in the system
s	Sub-channel s in the set S
$\boldsymbol{\mathcal{C}}$ ($\mathcal{U}$)	The set of groups (the set of ranks in each group)
$\mathcal{B}$	The set of small base stations in the network
u_{max}	The maximum number of MTDsin one group
$\gamma_{s,c,b}$	The binary indicator whether to allocate the s^{th} sub-channel to the c^{th} group to b^{th} SBS
$p_{s,m}$	The transmit power of the m^{th} MTDsover the s^{th} sub-channel
$\mathcal{N}_0$	AWGN
$\alpha_{m,u,c,b}$	The binary indicator whether to assign the m^{th} MTD to b^{th} SBS to the u^{th} rank of group c
$R_{m,b}$	The total transmission rate of the m^{th} MTD in the b^{th} SBS
W	The bandwidth of a single sub-channel in one PRB
$h_{s,m}$	The channel gain of the m^{th} MTD over the s^{th} sub-channel
R_m^{th}	The minimum transmission rate of the m^{th} MTD
P_m^{max}	The maximum power threshold of the m^{th} MTD

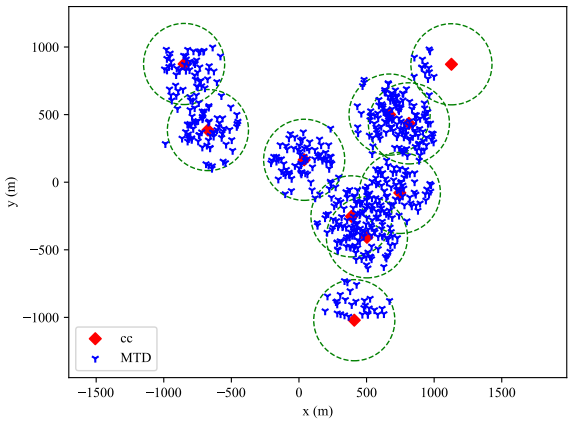

Fig. 1: Simulation of a Matérn cluster process

in each group is immune to other MTD's interference, while the other MTDs are subjected to interference from MTDs with higher ranks ($u = 2, ..., u_{\max}$). Furthermore, transmit power and QoS requirements are taken into account while analyzing intra-group interference [17]. PCP clustering uses the average channel gain of MTD, $\tilde{h}_m = \sum_{s \in \boldsymbol{\mathcal{S}}} \frac{h_{m,s}}{\boldsymbol{\mathcal{S}}}$. Then based on their $\tilde{h}_m$, they are assigned to the group with the next highest group rank.

To simplify what we mean by clustering process, and to be methodically accurate. The term clustering applies not only to how we group random sets of objects located in constrained space as shown in Fig. 2 (based on their proximity for example).

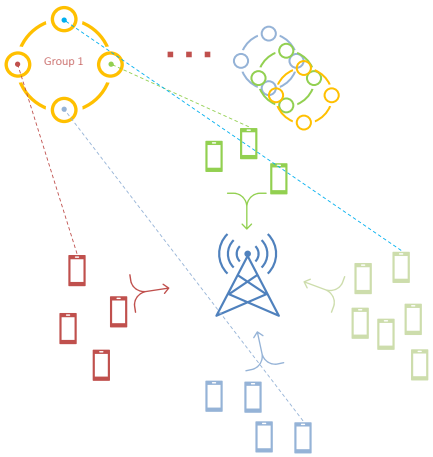

Fig. 2: Grouping MTDs based on their covariance

But also to higher levels of correlation in certain metrics. Hence, clustering in our study could mean two things, either how we initialize the location of MTDs based on PCP models as mentioned above. The other definition would be how to cluster MTDs for transmission. For example, suppose we have a group of MTDs that want to transmit on s sub-channel of $\boldsymbol{\mathcal{C}}_{\text{PD-NOMA}}$, the MTDs then will be clustered in groups that show the least correlation in their Channel State Information (CSI) after the first training (pilot) sequence is received the channel estimate is formulated with the combined knowledge of received signal and the pilot signal. Henceforth, the MTDs with the least similar CSI estimates will be clustered together, which will usually translate to different geographical positions. As demonstrated in [18], for MTD' positioning, the CSI signature should be both generally consistent in the same area and differentiable at various locations

III. Dynamic RRS Problem Formulation

A. Quality of Service Constraints

We start by defining $p_{m,s}$ as the m^{th} MTD's transmit power over the s^{th} sub-channel, and $\alpha_{m,c,u,b}$ as the binary variable used to allocate the m^{th} MTD to the u^{th} rank of group c. If there is scheduled, $\alpha_{m,c,u,b} = 1$, and zero otherwise. As a result, the MTD's achievable data rate R_m, The aggregate rate over the designated sub-channels for PD-NOMA groups over all SBS is shown in Eq.2. Consequently, with the assumption of no interference in OFDMA groups due to the nature of the access technique, which is robust against co-channel interference. The aggregate rate overall OFDMA groups for all SBSs, is shown below in Eq. 3

$$\boldsymbol{R}_{\text{PD-NOMA}} = \sum_{b \in \boldsymbol{\mathcal{B}}} \boldsymbol{R}_b = \sum_{\substack{c \in \\ \boldsymbol{\mathcal{C}}_{\text{PD-NOMA}}}} \sum_{u \in \mathcal{U}} \alpha_{m,c,u,b} \sum_{s \in \boldsymbol{\mathcal{S}}} \gamma_{s,c,b} W_1 \log_2 \left(1 + \frac{|h_{m,s}|^2 p_{m,s}}{\boldsymbol{\mathcal{N}}_0 W_1 + \sum_{h=u+1}^{u_{\max}} \alpha_d^{c,h} h_{d,s}^5 p_d^s}\right) \tag{2}$$

$$\boldsymbol{R}_{\text{OFDMA}} = \sum_{b \in \mathcal{B}} \boldsymbol{R}_b = \sum_{c \in \boldsymbol{\mathcal{C}}_{\text{OFDMA}}} \alpha_{m,c,b} \sum_{s \in \boldsymbol{\mathcal{S}}} \gamma_{s,c,b} W_2 \log_2 \left(1 + \frac{|h_{m,s}|^2 p_{m,s}}{\boldsymbol{\mathcal{N}}_0 W_2}\right) \tag{3}$$

where $h_{m,s}$ is the channel gain on sub-channel s between the m_{th} MTD and the SBS and $\mathcal{N}_0$ is the noise power spectral density. the m^{th} MTD experiences interference only from other higher ranked MTDs in the same group using the sub-channel.

To ensure that we have higher data rate than R_m^{th}'s minimum data rate, the following constraint is required

$$R_m^b \geqslant R_m^{th}, \quad \forall m \in \boldsymbol{\mathcal{M}} \ \& \ \forall b \in \mathcal{B}. \tag{4}$$

Furthermore, to discern between the minimum required data rates for devices accessing the medium either using PD-NOMA or OFDMA, the following constraints are considered to make sure the QoS requirements of either are met.

$$\begin{aligned} R_m^{\text{PD-NOMA}} &\geqslant {R_m^{\text{PD-NOMA}}}_{th}, \quad \forall m \in \boldsymbol{\mathcal{M}}, \\ R_m^{\text{OFDMA}} &\geqslant {R_m^{\text{OFDMA}}}_{th}, \quad \forall m \in \boldsymbol{\mathcal{M}}, \end{aligned} \tag{5}$$

The m^{th} MTD's overall transmit power is limited by its maximum power budget R_m^{th}, i.e.,

$$p_{m,s} \leqslant P_m^{\max}, \quad \forall m \in \boldsymbol{\mathcal{M}}. \tag{6}$$

B. Optimization Problem Formulation

The clustering-based OP for NB-IoT is described in this section as a sum rate maximization problem of MTD. In addition to the QoS requirements in Eq. (4), and Eq. (6), we should impose additional limitations for the PD-NOMA clustering process. Each MTD, in particular, should be assigned to only one group with a single rank, i.e.

$$\sum_{c \in \boldsymbol{\mathcal{C}}} \sum_{u \in \mathcal{U}} \alpha_{m,c,u,b} = 1, \quad \forall m \in \boldsymbol{\mathcal{M}}, \tag{7}$$

Because the purpose of PD-NOMA is to share spectral resources among multiple MTD, the PD-NOMA grouping en-

forces the presence of more than one MTD in each group, i.e., the same applies to OFDMA groups as we consider inter-cell interference, but in this equation we chose to disregard inter-cell interference

$$\sum_{m\in\boldsymbol{\mathcal{M}}}\sum_{u\in\mathcal{U}}\alpha_{m,c,u,b}\geqslant 2,\quad \forall c\in\boldsymbol{\mathcal{C}}_{\text{PD-NOMA}}. \tag{8}$$

$$\sum_{m\in\boldsymbol{\mathcal{M}}}\sum_{u\in\mathcal{U}}\alpha_{m,c,u,b}\geqslant 2,\quad \forall c\in\boldsymbol{\mathcal{C}}_{\text{OFDMA}}. \tag{9}$$

and we guarantee the priority of rank assignment in each group by starting with the lowest rank in each group ($u=1$), i.e.,

$$\alpha_{m,c,u,b}\leqslant\alpha_{m,c,u-1},\ \forall m\in\boldsymbol{\mathcal{M}},\ \forall c\in\boldsymbol{\mathcal{C}},\ 2\leqslant u\leqslant u_{\max}, \tag{10}$$

Finally, the sum-rate maximization of MTDs transceiving over OFDMA and PD-NOMA channels can be formulated as joint scheduling and sub-channel allocation multi-objective OP below

$$\underset{p_{m,s},\alpha_{m,c,u,b},\gamma_{s,c,b}}{\text{maximize}}\quad(\boldsymbol{R}_N,\boldsymbol{R}_O) \tag{11a}$$

subject to

$$R_m\geqslant R_m^{th},\quad\forall m\in\boldsymbol{\mathcal{M}}, \tag{11b}$$

$$R_m^{\text{PD-NOMA}}\geqslant R_m^{\text{PD-NOMA}_{th}},\quad\forall m\in\boldsymbol{\mathcal{M}}, \tag{11c}$$

$$R_m^{\text{OFDMA}}\geqslant R_m^{\text{OFDMA}_{th}},\quad\forall m\in\boldsymbol{\mathcal{M}}, \tag{11d}$$

$$p_{m,s}\leqslant P_m^{\max},\quad\forall m\in\boldsymbol{\mathcal{M}}, \tag{11e}$$

$$p_{m,s}>0,\quad\forall m\in\boldsymbol{\mathcal{M}},\quad\forall s\in\boldsymbol{\mathcal{S}}, \tag{11f}$$

$$\alpha_{m,c,u,b}\leqslant\alpha_{m,c,u-1},\ \forall m\in\boldsymbol{\mathcal{M}},\ \forall c\in\boldsymbol{\mathcal{C}},\ 2\leqslant u\leqslant u_{\max}, \tag{11g}$$

$$\sum_{c\in\boldsymbol{\mathcal{C}}}\sum_{u\in\mathcal{U}}\alpha_{m,c,u,b}=1,\quad\forall m\in\boldsymbol{\mathcal{M}}, \tag{11h}$$

$$\sum_{m\in\boldsymbol{\mathcal{M}}}\sum_{u\in\mathcal{U}}\alpha_{m,c,u,b}\geqslant 2,\quad\forall c\in\boldsymbol{\mathcal{C}}_{\text{PD-NOMA}}, \tag{11i}$$

$$\sum_{m\in\boldsymbol{\mathcal{M}}}\sum_{u\in\mathcal{U}}\alpha_{m,c,u,b}\geqslant 2,\quad\forall c\in\boldsymbol{\mathcal{C}}_{\text{OFDMA}}, \tag{11j}$$

$$\sum_{s\in\boldsymbol{\mathcal{S}}}\sum_{c\in\boldsymbol{\mathcal{C}}}\gamma_{s,c,b}\boldsymbol{\mathcal{W}}_{s,c,b}\leqslant W^{RB},\quad\forall c\in\boldsymbol{\mathcal{C}},\quad\forall s\in\boldsymbol{\mathcal{S}}, \tag{11k}$$

$$\gamma_{s,c,b}\in\{0,1\},\quad\forall c\in\boldsymbol{\mathcal{C}},\quad\forall s\in\boldsymbol{\mathcal{S}}, \tag{11l}$$

$$\alpha_{m,c,u,b}\in\{0,1\},\quad\forall m\in\boldsymbol{\mathcal{M}},\quad\forall c\in\boldsymbol{\mathcal{C}},\quad\forall u\in\mathcal{U} \tag{11m}$$

where the constraints are considered as follows, (11b) requires MTDs to have data rates greater than a data rate threshold requirement. (11c) requires MTDs using PD-NOMA to have a data rate greater than the minimum threshold PD-NOMA data rate. The same applies for (11d) which instead specifies a minimum data rate requirement for MTDs using OFDMA for transmissions.

The m^{th} MTD total transmit power is restricted to the max power allocation by (11e), P_m^{max} available. (11f) restricts MTDs transmit powers to positive values. (11g) suggest that MTDs can be assigned to the u^{th} rank of the c^{th} group if all lower ranks have been assigned to other MTD. (11h) is designed to guarantee that each device (MTD) is allocated to just one group and one rank within that group. (11i) and (11j) are to ensure that there is more than one member in each PD-NOMA and OFDMA group. (11k) ensures that the total bandwidth allotted to all PCP groups does not exceed one RB (bandwidth of one RB in NB-IoT is 180 kHz). (11l) and (11m) verify that the variables $\gamma_{s,c,b}$, $\alpha_{m,c,u,b}$, and are only permitted to have binary values.

1) NP-Hardness of OP(11): The general Eq. (11) is an NP-Hard Problem. the OP(11) scheduling part is identical to the Makespan job shop scheduling problem where we want to execute n jobs (data transmission $\alpha_{m,c,u,b}$) by i identical ($\boldsymbol{\mathcal{S}}_b^c$) (sub-channels), which is by definition a combinatorial NP-Hard problem [19].

Similarly, the resource allocation part is analogous to a Multi-Choice Multiple Knapsack Problem (MCMKP), as we are attempting to fit $\boldsymbol{\mathcal{M}}$ items into $\boldsymbol{\mathcal{S}}_c^b$ knapsacks (sub-channels), which is also an NP-Hard problem.

2) Solution to OP(11): WLOG, we relax the power constraints for both PD-NOMA and OFDMA MTD. We assume the MTDs transmit using a predetermined powers $p_{s,m}=P_{s,m}^{max}-\frac{u_{m,c,b}}{P_{s,m}^{step}}$, thus the power-related constraints can be relaxed. In order to simplify the problem further, we apply linear scalarization, which is a priori method, where solving the single-objective OP formed from a multi-objective problem means that the optimal solutions of the single OP are Pareto optimal solutions to the multi-objective OP, the Pareto optimality could be attained by adjusting the weight of scalarization ω_N [20]. Finally, we propose a heuristic solution in the form of a distributed alternating convex optimization problem (DCOP) with two secondary optimization problems. Where the goal for the the first SOP12 is to maximize R subject to scheduling constraints of $\alpha_{m,c,u,b}$, which will feed its optimal scheduling to SOP13 whose goal is to maximize R subject to sub-channel $\gamma_{m,s,u,b}$ allocation constraints. We denote the resource distribution with ω_N, Therefore, SOP1 is formulated as follows:

$$\underset{\alpha_{m,c,u,b}}{\text{maximize}}\quad\sum_{i=1}^{k}(\omega_{Ni}R_{Ni}+(1-\omega_{Ni})R_{Oi}) \tag{12a}$$

$$\text{subject to}\quad 11b-11d,11g-11j,11m, \tag{12b}$$

$$\omega_N\in(0,1],\forall\omega_N\in\Omega, \tag{12c}$$

(12c) bounds the weight of allocated resources of $R_{\text{PD-NOMA}}$ over R_{OFDMA} and vice versa, ω_N therefore is between 0 and 1. Respectively, SOP2 is formulated as follows,

$$\underset{\gamma_{s,c,b}}{\text{maximize}}\quad\sum_{i=1}^{k}(\omega_{Ni}R_{Ni}+(1-\omega_{Ni})R_{Oi}) \tag{13a}$$

$$\text{subject to}\quad\sum_{s\in\boldsymbol{\mathcal{S}}}\gamma_{s,c,b}=1,\quad\forall c\in\boldsymbol{\mathcal{C}}, \tag{13b}$$

$$11k,11l, \tag{13c}$$

$$\omega_N \in (0, 1], \forall \omega_N \in \Omega, \tag{13d}$$

where each sub-channel cannot be assigned to more than one group, according to (13b). The formulated OP1 is an NP-Hard non-convex mixed integer non-linear program (MINLP), which is combinatorial in nature, accordingly, the heuristic solution proposed above can be used to solve OP(11).

IV. Simulation Results

In this section, we present our simulation results the results accuracy is validated using Monte Carlo simulations with up 10^3 iterations for each scenario with 5×10^4 different scenarios. Henceforth, we will discuss which hyper-parameters of the simulation had the most consequential impact on the sum-rate maximization. To construct the Pareto dominance rank plot, the main parameter to tune is ω_N (which represents, in our case, the resource allocations given to MTDs using OFDMA or PD-NOMA). The effect of changing ω_N results in a Pareto frontier

TABLE II: Simulation Hyper-parameters

Definition	Value
Parent points density	$\{ \lambda_{\mathrm{p}_u}: 10 \leqslant \lambda_{\mathrm{p}_u} \leqslant 200\}$
The cluster radius of Parent point process	$\{ r_c: 1000 \text{ m} \geqslant \mathrm{r}_c \geqslant 200 \text{ m}\}$
Daughter points density	$\{ \mathcal{D}_u : 100/\mathrm{km}^2 \leqslant \mathrm{D}_u \leqslant 20000/\mathrm{km}^2\}$
Path Loss Model (Macro-cell propagation model)	$L = 128.1 + 37.6 \log_{10}(d)$, d in km
Transmit power step	$P_{s,m}^{step} = 10000$
The maximum power threshold of the m^{th} MTD	$P_m^{max} = 0.1\ mW$
The bandwidth of a single sub-channel in one PRB	$W = 15\ kHz$
The MTD antenna gain of the m^{th} MTD over the s^{th} sub-channel	$\{G_{s,m}: 0 \text{ dB} \leqslant \mathrm{G}_{s,m} \leqslant 10 \text{ dB}\}$
The noise figure of the m^{th} MTD over the s^{th} sub-channel	$NF_{m,s} = 9\ dB$
Sample size (per experiment step)	$10 \leqslant \mathrm{n} \leqslant 1000$

for each scenario, from which we can draw the following conclusions. The maximum achievable sum-rate (where PD-NOMA MTDs are given the same resources as OFDMA MTD) occurs at $\omega_N = 0.5$, as shown in Fig. 3 (100 MTD/group). In the same figure the total sum-rate of both PD-NOMA and OFDMA curves is shown, which clearly translates the effect of varying ω_N over the total sum-rate of the all devices in that particular scenario. Furthermore, using a Monte Carlo method, we arrive empirically at the conclusion that $\omega_N = 0.566$.

Therefore, PD-NOMA MTD's Sum-Rate will cross with the OFDM's at a much higher ω_N as we increase the group size.

Subsequently, we can observe in PD-NOMA vs. OFDMA Pareto dominance rank plots as shown in Fig. 4 we can see that as we reduce the interference level, we achieve a much larger capacity region. That above conclusion remains consistent even with different-sized groups. Similarly, Fig. 5, showcases that as we decrease the cluster radius, we achieve a much higher sum-rate for both PD-NOMA and OFDMA.

This conclusion is enriched as we look at the capacity region plots of PD-NOMA vs. OFDMA, where we can observe a clear trend towards reducing the generated MTD's cluster

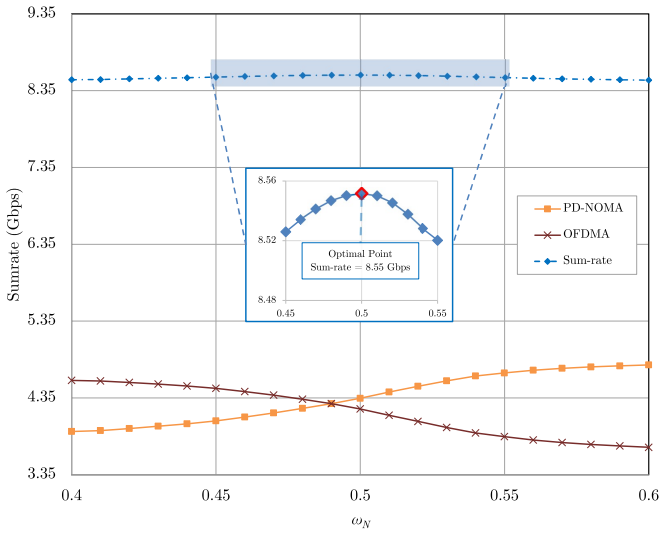

Fig. 3: Sum-rate performance for variable ω_N (PD-NOMA & OFDMA sum-rate vs Total sum-rate)

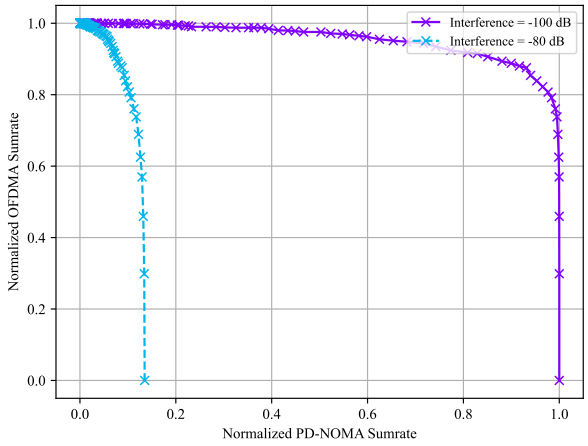

Fig. 4: Pareto dominance rank plot (Normalized Intra-group Interference effect on maximum sum-rate)

radius. This result is due to how the algorithm is designed. The way it works, as we increase the cluster radius, MTDs are still going to be generated in a limited scaled space, meaning that their channel correlation will get higher as we increase the cluster radius, and even if we decide to pick the users with the least correlation in the same group, we will observe that this decision, which is one of the prime reasons for improving the overall spectral efficiency of the MTDs in the same group, is minimal. Further experimentation while varying SBSs' scheduling capacity showcased in certain scenarios that the best 500 MTDs have a on average a sumrate of 5.91 Gbps, while if we schedule all MTDs we only achieve

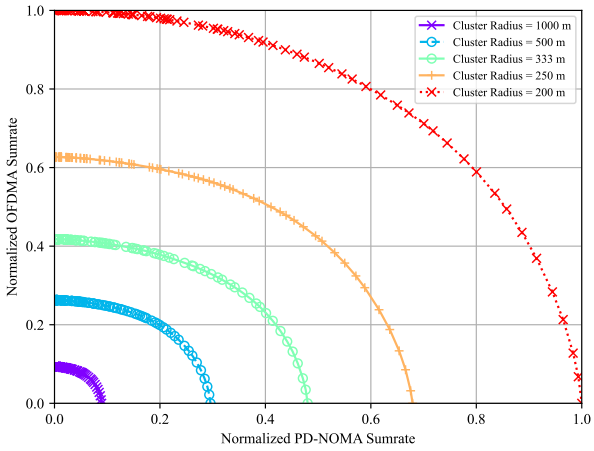

Fig. 5: Pareto dominance rank plot (Normalized cluster radius effect on maximum rate)

a 7.60 Gbps, which is a mere improvement of 28.59 % as we allow for ten times more MTDs to transmit to the SBS. We can say that, on average, 500 MTDs (which are the highest ranks in their respective groups) and 10% of all MTDs in the simulation achieve 77.76% of the maximum achievable rate of the connected MTDs.

V. Conclusions and Future Work

In this paper, we present a perspective on how backward compatibility could look in the near future. We formulate a joint scheduling and resource allocation optimization problem for a HetNet mMTC scenario. We then propose a heuristic solution to a relaxed OP. We finally come to a conclusion that certain hyper-parameters have a tangible impact on the maximum achievable sum-rate. A promising extension to this work is by using Deep Reinforcement Learning algorithms (DRL) i.e., actor-critic and policy-based methods to solve the non-relaxed problem. We hypothesize that DRL is going to be a primary solving tool for current and next-gen telecommunication networks paradigms.

Acknowledgement

This work was supported by Qatar University Grants M-QJRC-2020-4 and QUHI-CENG-21/22-1. This research is also supported by a grant from the Natural Sciences and Engineering Research Council of Canada (NSERC) under Grant Number STPGP 521432-2018. The statements made herein are solely the responsibility of the authors.

References

[1] S. Alraih *et al.*, "Revolution or Evolution? Technical Requirements and Considerations towards 6G Mobile Communications," *Sensors*, vol. 22, no. 3, p. 762, Jan. 2022, number: 3 Publisher: Multidisciplinary Digital Publishing Institute.

[2] N. H. Mahmood *et al.*, "Machine type communications: key drivers and enablers towards the 6G era," *EURASIP Journal on Wireless Communications and Networking*, vol. 2021, no. 1, p. 134, Jun. 2021.

[3] N. Abu-Ali, A.-E. M. Taha, M. Salah, and H. Hassanein, "Uplink Scheduling in LTE and LTE-Advanced: Tutorial, Survey and Evaluation Framework," *IEEE Communications Surveys Tutorials*, vol. 16, no. 3, pp. 1239–1265, 2014.

[4] K. Sridevi and M. A. Saifulla, "Control Plane Efficiency by Load Adjustment in SDN," in *Smart Trends in Computing and Communications*, ser. Lecture Notes in Networks and Systems, Y.-D. Zhang, T. Senjyu, C. So-In, and A. Joshi, Eds. Singapore: Springer, 2022, pp. 515–524.

[5] C.-W. Huang, S.-C. Tseng, P. Lin, and Y. Kawamoto, "Radio Resource Scheduling for Narrowband Internet of Things Systems: A Performance Study," *IEEE Network*, vol. 33, no. 3, pp. 108–115, 2019.

[6] Y. Xu, G. Gui, H. Gacanin, and F. Adachi, "A Survey on Resource Allocation for 5G Heterogeneous Networks: Current Research, Future Trends, and Challenges," *IEEE Communications Surveys Tutorials*, vol. 23, no. 2, pp. 668–695, 2021, conference Name: IEEE Communications Surveys Tutorials.

[7] P. Trakas, F. Adelantado, N. Zorba, and C. Verikoukis, "A QoE-Aware Joint Resource Allocation and Dynamic Pricing Algorithm for Heterogeneous Networks," in *GLOBECOM 2017 - 2017 IEEE Global Communications Conference*, 2017, pp. 1–6.

[8] D. J. Langley *et al.*, "The internet of everything: Smart things and their impact on business models," *Journal of Business Research*, vol. 122, pp. 853–863, 2021.

[9] P. Jain and P. Kar, "Non-convex optimization for machine learning," *Foundations and Trends® in Machine Learning*, vol. 10, no. 3-4, p. 142–336, 2017, publisher: Now Publishers.

[10] E. C. Cejudo, H. Zhu, and J. Wang, "Resource Allocation in BER-Constrained Multicarrier NOMA Based on Optimal Channel Gain Ratios," in *2021 IEEE Global Communications Conference (GLOBECOM)*, Dec. 2021, pp. 1–6.

[11] P. Semasinghe, S. Maghsudi, and E. Hossain, "Game Theoretic Mechanisms for Resource Management in Massive Wireless IoT Systems," *IEEE Communications Magazine*, vol. 55, no. 2, pp. 121–127, Feb. 2017, conference Name: IEEE Communications Magazine.

[12] N. Zorba and A. I. Perez-Neira, "Robust power allocation schemes for multibeam opportunistic transmission strategies under quality of service constraints," *IEEE Journal on Selected Areas in Communications*, vol. 26, no. 6, pp. 1025–1034, 2008.

[13] A. Celik, A. Chaaban, B. Shihada, and M.-S. Alouini, "Topology Optimization for 6G Networks: A Network Information-Theoretic Approach," *IEEE Vehicular Technology Magazine*, vol. 15, no. 4, pp. 83–92, 2020.

[14] H. Al-Obiedollah, H. B. Salameh, S. Abdel-Razeq, A. Hayajneh, K. Cumanan, and Y. Jararweh, "Energy-efficient opportunistic multi-carrier NOMA-based resource allocation for beyond 5G (B5G) networks," *Simulation Modelling Practice and Theory*, vol. 116, p. 102452, 2022.

[15] A. Shahini and N. Ansari, "NOMA aided narrowband IoT for machine type communications with user clustering," *IEEE Internet of Things Journal*, vol. 6, no. 4, pp. 7183–7191, 2019.

[16] C. Saha, M. Afshang, and H. S. Dhillon, "Poisson cluster process: Bridging the gap between PPP and 3GPP HetNet models," in *2017 Information Theory and Applications Workshop (ITA)*, 2017, pp. 1–9.

[17] N. Zorba and A. I. Pérez-Neira, "Cac for multibeam opportunistic schemes in heterogeneous wimax systems under qos constraints," in *IEEE GLOBECOM 2007-IEEE Global Telecommunications Conference*. IEEE, 2007, pp. 4296–4300.

[18] Z. Wu *et al.*, "Accurate indoor localization based on CSI and visibility graph," *Sensors*, vol. 18, no. 8, p. 2549, 2018.

[19] D. Applegate and W. Cook, "A computational study of the job-shop scheduling problem," *ORSA Journal on computing*, vol. 3, no. 2, pp. 149–156, 1991.

[20] A. Ghane-Kanafi and E. Khorram, "A new scalarization method for finding the efficient frontier in non-convex multi-objective problems," *Applied Mathematical Modelling*, vol. 39, no. 23, pp. 7483–7498, 2015.